

## Research article

Giulia Guidetti, Guy Levy, Giusy Matzeu, Joshua M. Finkelstein, Michael Levin  
and Fiorenzo G. Omenetto\*

# Unmixing octopus camouflage by multispectral mapping of *Octopus bimaculoides*' chromatic elements

<https://doi.org/10.1515/nanoph-2021-0102>

Received March 10, 2021; accepted May 27, 2021;  
published online June 18, 2021

**Abstract:** Cephalopods camouflage abilities arise from highly specialized chromatic elements in their skin, chromatophores, iridophores, and leucophores, that enable them to display complex and rapidly changing color patterns. Despite the extensive study of these chromatic elements in squid and cuttlefish, full characterization of their individual optical response is still elusive in the *Octopus* species. We present here detailed multispectral analysis and mapping of the *Octopus bimaculoides* skin that allows to precisely identify the spatial distribution of the animal's pigmented and structural elements. The mutual interaction of chromatophores and iridophores is also characterized both in terms of spectral response and spatial localization. The spectral information obtained through this analysis

helps to understand the complexity and behavior of these natural tissues while continuing to serve as an inspiration for the fabrication of advanced, chromatically adaptable materials.

**Keywords:** biophotonics; dynamic coloration; multispectral mapping; *Octopus bimaculoides*.

## 1 Introduction

Octopuses are ingenious coleoid cephalopods that exhibit some of the most spectacular color patterns and camouflage abilities of the animal kingdom [1, 2]. Similarly to squid and cuttlefish, they can rapidly (~ms) change their body pattern to match the brightness of their surroundings for camouflage and communication purposes by neurally controlling the chromatic elements in their skin [2–4]. The displayed body patterns arise from the hierarchical organization of the skin whose color and texture derive from the combination of the optomechanical response of highly specialized classes of organs and cells; specifically, the skin contains vertically stacked chromatic elements that can generate color either through pigmentation, the chromatophores, or through interference with visible light, iridophores, and leucophores (Figure 1). Chromatophores are traditionally described as selective absorbing filters responsible for long wavelength colors such as yellow, red, and brown [5–10]. Their displayed color is thought to depend on the oxidation state of tethered pigment granules present in the elastic sacculus and on the sacculus conformation which can be either expanded or punctuated depending on the relaxation status of radial muscles directly innervated to the brain [7, 11]. Iridophores work as selective reflective filters due to the presence of 1D photonic stacks, the iridocytes, formed by the regular alternation of layers of reflectin and cytoplasm at the nanoscale that create the index contrast necessary for selective reflection [9, 10, 12, 13]. These structures reflect colors spanning from blue to red depending on the relative thickness of each layer. Finally, the leucophores display a

\*Corresponding author: Fiorenzo G. Omenetto, Silklab, Department of Biomedical Engineering, Tufts University, Medford, MA, 02155, USA; Laboratory for Living Devices, Tufts University, Medford, MA, 02155, USA; Department of Physics, Tufts University, Medford, MA, 02155, USA; and Department of Electrical and Computer Engineering, Tufts University, Medford, MA, 02155, USA,  
E-mail: fiorenzo.omenetto@tufts.edu. <https://orcid.org/0000-0002-0327-853X>

Giulia Guidetti and Giusy Matzeu, Silklab, Department of Biomedical Engineering, Tufts University, Medford, MA, 02155, USA; and Laboratory for Living Devices, Tufts University, Medford, MA, 02155, USA, E-mail: giulia.guidetti@tufts.edu (G. Guidetti), giusy.matzeu@tufts.edu (G. Matzeu). <https://orcid.org/0000-0002-6065-3359> (G. Guidetti). <https://orcid.org/0000-0002-5218-5866> (G. Matzeu)

Guy Levy and Michael Levin, Department of Biology, Tufts University, Medford, MA, 02155, USA; and Allen Discovery Center, Tufts University, Medford, MA, 02155, USA, E-mail: guy.levy@tufts.edu (G. Levy), Michael.Levin@tufts.edu (M. Levin). <https://orcid.org/0000-0001-6807-4004> (G. Levy). <https://orcid.org/0000-0001-7292-8084> (M. Levin)

Joshua M. Finkelstein, Allen Discovery Center, Tufts University, Medford, MA, 02155, USA, E-mail: jmfinkelstein@gmail.com. <https://orcid.org/0000-0003-2613-9345>

broadband scattering response due to the presence of disordered reflectin granules [14, 15]. Typically, chromatophores occupy the outermost layer in the octopus skin, with lighter chromatophores being more superficial than darker ones, while iridophores and leucophores are localized deeper in the skin [2, 16].

Among the many species of octopus documented so far [17], *Octopus bimaculoides* [18] is of particular interest as its limited size and temperate growing environment makes it ideal to be bred and studied in laboratory conditions [16, 19, 20]. *O. bimaculoides* inhabits the Pacific Ocean and can be found up to 30 m deep living in muddy bottoms with rocky dens [21, 22]. Its anatomy is well known [23, 24] and its genome drives expression of specialized cephalopod-related functions including skin, nervous system and suckers [25]. *O. bimaculoides* vision [26] and response to odors [27] have been studied together with temperamental traits [28], learning skills [29–31], and the skin ability to perform distributed light sensing [32]. In spite of the *O. bimaculoides* body patterns (the appearance of the

whole animal) being documented [2, 16], the optical and spectroscopic response of the individual chromatic elements (the chromatic organs in the skin constituting the building blocks of the body patterns) has not been yet extensively studied.

Comprehensive microspectroscopic studies of complex natural dynamic systems, such as the octopus skin, are nontrivial as they require to capture the rich optical response of a material that displays both dynamic pigmentary and structural coloration (Figure 1(A)). Multispectral mapping is a spectral imaging technique that consists in the collection of three-dimensional optical image cubes ( $x$ ,  $y$ , and  $z$ , with  $x$  and  $y$  accounting for the spatial dimensions and  $z$  for the spectral dimension, for a wavelength range  $\lambda_{\text{start}}-\lambda_{\text{end}}$  with a step size  $\Delta\lambda$ ) that contain spectral information for every pixel of the image (Figure 1(B)) [33, 34]. For cephalopods, multispectral mapping allows for the spatial localization of each of the chromatic element class which displays a specific spectral response (Figure 1(C)). Of the octopus' chromatic elements

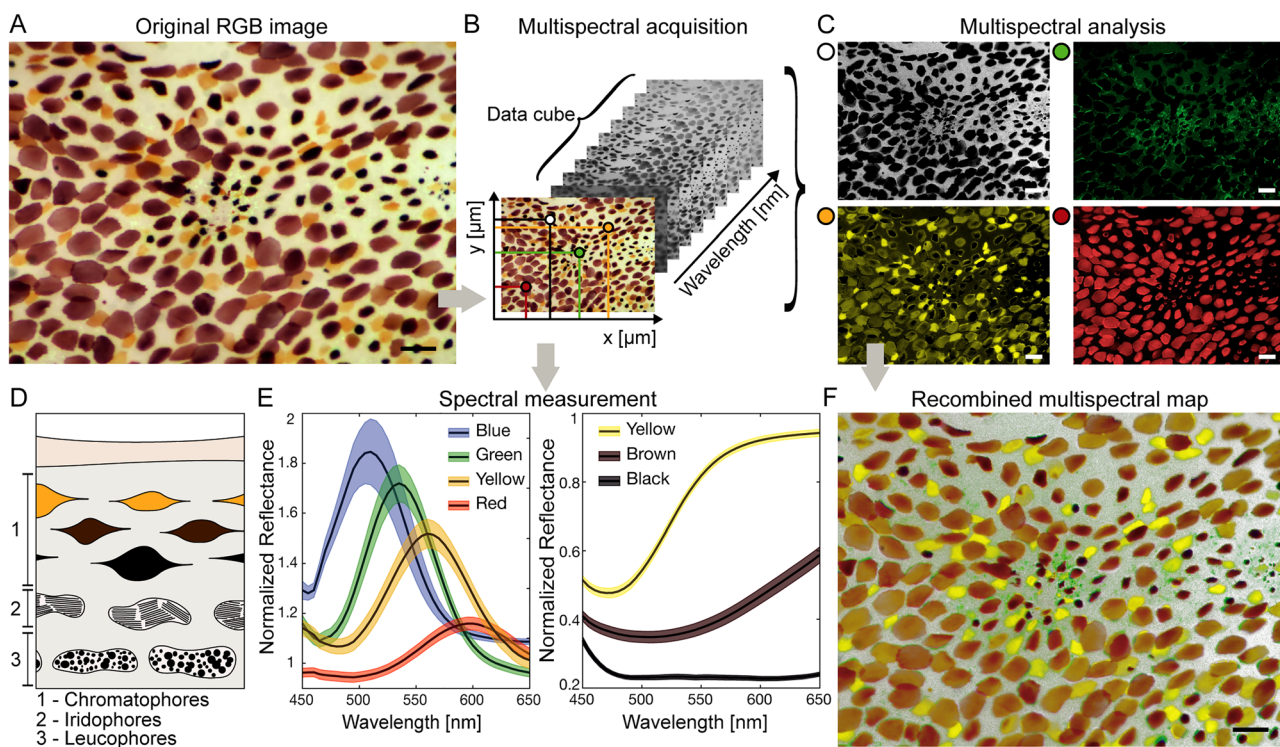


**Figure 1:** Multispectral analysis of octopus skin.

(A) The original RGB brightfield reflectance image of the octopus skin is part of the (B) multispectral acquisition of the skin, which consists in a data cube of the reflectance response within a specific wavelength range for every pixel of the image. The multispectral analysis allows to (C) isolate the spectral response or relevant optical elements of the skin, in this case belonging to (D) the chromatophores (yellow and brown dots), the iridophores (green dot), and the bare skin (white dot), which are labeled according to (E) their average reflectance as a function of wavelength. The reflectance spectra are normalized with respect to the response of a region of the skin with no chromatophore/iridophore and the shaded regions correspond to the standard error of the mean. The combination of the (C) individual spectral maps leads to the (F) recombined multispectral map. Scale bar: 200  $\mu\text{m}$ .

(Figure 1(D)), the iridophores and chromatophores classes are spectrally labeled (Figure 1(E)) and taken into account to obtain the recombined multispectral map (Figure 1(F)). The multispectral mapping technique has also been used to predict the visual appearance of cuttlefish as seen by the eyes of different predators [33], complementing the spectral analysis of its body patterns and surroundings performed in its natural habitat [35].

Here we map the spectral response of *O. bimaculoides*' skin using multispectral imaging. Multispectral mapping of the skin allows first to spatially and spectrally discriminate the chromatic elements of both fresh and aged skin; it then provides insights on pigment distribution within individual chromatophores, and, finally, it assesses the interplay of the different chromatic elements. These findings enable a spectrally resolved topographical mapping of the cephalopod chromatic elements both as classes and as individual elements. In addition to providing further understanding of the chromatic elements' optical response, these findings are applicable for the design of chromatically adaptable materials.

## 2 Materials and methods

### 2.1 Materials

Artificial sea water (ASW) at 35‰ salinity with  $[MgCl_2] = 55\text{ mM}$  was prepared by dissolving salts powder (Instant Ocean) in double deionized water to match the salinity of *O. bimaculoides* natural habitat (34–37‰ [36]). Sodium L-glutamate monohydrate solution at 500 mM was prepared by dissolving the powder (TCI Chemicals) in deionized (DI) water. Silk fibroin was extracted from the silk cocoons of the *Bombyx mori* silkworm following a previously described protocol [37]. Briefly, cocoons were cut in small pieces, boiled for 30 min in 0.02 M  $Na_2CO_3$  aqueous solution, and rinsed thoroughly with distilled water in order to remove the sericin. The extracted silk fibroin fibers were dissolved in a 9.3 M LiBr solution at 60 °C for 4 h. After that, the solution was dialyzed against DI water using a dialysis membrane (Fisherbrand, MWCO 3.5 kDa) for two days, followed by centrifugation at 10,000 rpm (Beckman Coulter, Allegra X-14, FX6100) and the clear supernatant was then collected, filtered, and stored at 4 °C. The solution was concentrated to 13 wt. % using a dialysis membrane (Fisherbrand, MWCO 3.5 kDa). All chemicals were used without further purification.

### 2.2 Animal handling

Wild caught specimen of live *O. bimaculoides* was purchased from Aquatic Research Consultants. The reported optical analysis was performed on the skin taken from the tentacles of one individual male octopus (weight = 77.1 g) collected in the California Bay region (Long beach harbor) in winter. To ensure consistency with previously reported studies, the AAALAC (Association for Assessment and Accreditation of Laboratory Animal Care) guidelines were followed for handling

octopuses and administering anesthesia [38]. Upon receipt, the animals were progressively acclimatized in ASW for ~1 h, at room temperature ( $T = 20\text{ }^{\circ}\text{C}$ ). The animals were then immersed in the anaesthetic solution (ASW with  $[MgCl_2] = 110\text{ mM}$  and 2% v/v ethanol [38–40]) for at least 15 min and sectioned once dead. Individual arms were rinsed with fresh ASW and stored in ASW at 35‰ salinity at 4 °C until further use. The outer skin and flesh layers were separated by the internal fleshy layer by dissection. During the dissection the arms were kept hydrated in ASW and the separated skin tissue was stored in ASW until further use. Unless otherwise specified, the skin was used as it was and kept wet with ASW during the optical analysis. To perform optical microscopy of the fresh skin, the excised skin was stabilized by immersion in 13 wt. % silk fibroin solution and in 100 mM sodium glutamate to minimize the muscular movement and the chromatophores pulsing [6, 41, 42]. The skin was considered to be fresh when analyzed within 24 h from excision, while aged when analyzed at  $24\text{ h} < t_{from\ excision} < 48\text{ h}$ . No significant difference was observed between the skin taken from different tentacles, thus, in agreement with existing cephalopod literature [10, 25], the number of individuals was minimized and the amount of skin from each studied arm was maximized.

### 2.3 Optical microscopy and spectroscopy

Optical microscopy and spectroscopy were performed using two customized setups. For low magnification images (1–6.3 $\times$ ) an Olympus SZ STU-2 stereo microscope equipped with a multispectral camera (CRI Nuance FX) and an illuminator (Edmund Optics, MI-150) was used; for higher magnification images (10–20 $\times$ ) an Olympus Inverted IX71 microscope equipped with a multispectral camera (CRI Nuance EX) and with a halogen lamp (Olympus, U-LH100L-3) as light source was used. Bright field reflection images were collected using 10 $\times$  (Olympus, UPlanFL N NA 0.3) and 20 $\times$  (Olympus, LUCPlanFL N, NA 0.45) objectives. The spectral maps were acquired in the ranges 450–720 nm (acquisition time = 20–45 s) with a step size of 5 nm, with the exception of the map reported in Figure 2 which was acquired in the 450–650 nm interval with the same step size (acquisition time = 2 s). The intensity of the microscopes illumination sources and the multispectral cameras exposure were adjusted to minimize the time required to acquire individual multispectral maps. The software Nuance 3.0.2 was used to acquire the multispectral maps and the software MATLAB R2020a and Fiji were used to analyze the data. Specifically, the multispectral maps were analyzed after acquisition to isolate the RGB image, identify the relevant spectral responses, unmix the multispectral map according to those spectral responses, and build the recombined image. To take into account the natural variation of the iridophores and of the chromatophores within the same animal, reflectance spectra were acquired from different individual chromatic elements in the studied skin regions and used to assign chromatic elements to each class as reported in Figure 1(E). Specifically, the average bright field reflectance spectra of iridophores and chromatophores reported in Figure 1(E) were calculated from  $n$  different chromatic elements as it follows: for the iridophores  $n_{blue} = 12$ ,  $n_{green} = 14$ ,  $n_{yellow} = 10$ , and  $n_{red} = 20$ ; for the chromatophores  $n_{black} = 40$ ,  $n_{brown} = 20$ , and  $n_{yellow} = 40$ . The spectra reported in Figure 1(E) have been normalized to the reflectance signal of a region of the skin with no chromatophores/iridophores to better distinguish the differences in the reflectance intensity between pigmented and structural elements. The spectra reported in all other figures have been normalized with respect to each curve's maximum. For the multispectral maps of the aged skin the background signal was unmixed into white (false color) and used to

compute the combined false color multispectral map. The number of individual spectral classes identified for chromatophores for each multispectral map was determined as a function of significative differences in their spectral response with the aim of minimizing the number of spectrally different classes in light of what recently reported for other cephalopods [42], except for what reported in Figure 3. In this case, the number of spectrally different chromatophore classes was maximized with the aim to demonstrate how multispectral mapping can be used to infer information on the chromatophores pigment density distribution.

### 3 Results

#### 3.1 Chromatic elements assignment

The chromatic elements of the cephalopod skin were classified as chromatophores or iridophores by visual inspection in combination with spectroscopic measurements (Figure 1 and S1) based on, respectively, morphological and optical similarities with previously reported chromatic elements for *O. bimaculoides* and for cephalopods in general [2, 9, 32]. In particular, the observed presence of high circularity and pulsing elements identifies the elements as

pertaining to the chromatophore class while iridescent, strongly reflecting, and size invariant elements were identified as iridophores. In addition, the area of the iridophores is considerably smaller ( $2\text{--}20 \mu\text{m}^2$ ) than the one of the chromatophores ( $900\text{--}12000 \mu\text{m}^2$ ), regardless of the chromatophores expansion state, consistent with previously reported results [9]. As the leucophores do not generate coloration by themselves but uniformly scatter the light impinging on them, they were not considered for the multispectral mapping performed.

#### 3.2 Excised stabilized fresh skin

Freshly excised skin (<24 h from excision) was observed to display both muscular movement and chromatophores pulsing which complicates its optical analysis thus leading to studies of the chromatic response *ex vivo* that report on the expansion and contraction (i.e., punctuation) of chromatophores following a wave pattern without correlation to any specific external stimuli [5, 6, 32].

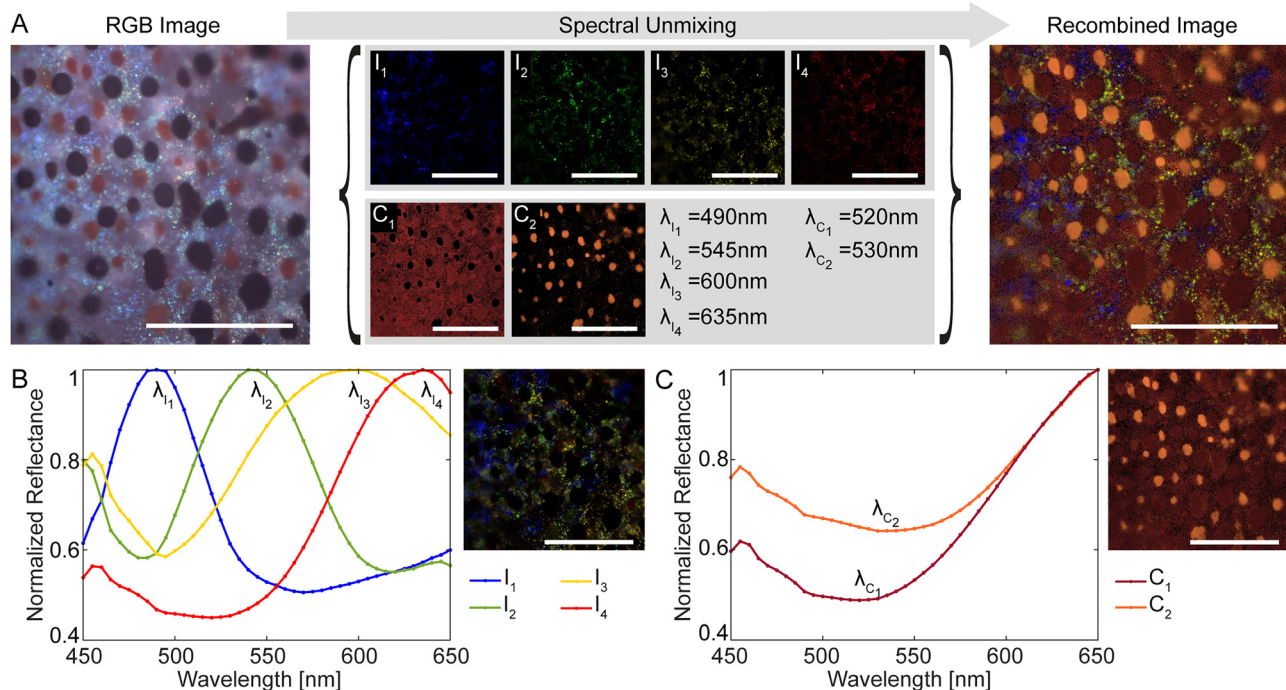


**Figure 2:** Multispectral map of freshly excised, stabilized *Octopus bimaculoides* skin.

(A) The RGB image of freshly excised stabilized *Octopus bimaculoides* skin is spectrally unmixed in false-color images that show the spatial distribution of the iridophores (Spectral Unmixing  $I_1\text{--}I_4$ ) and of the chromatophores (Spectral Unmixing  $C_1\text{--}C_2$ ) in the spectral range 450–650 nm. The recombination of the individual spectral bands generates a false-color composite image showing the chromatic elements' spatial distribution (Recombined Image). The iridophores' spectral response is identified by their reflectance maximum ( $\lambda_{I_1}\text{--}\lambda_{I_4}$ ), while the chromatophores' by their reflectance minimum ( $\lambda_{C_1}\text{--}\lambda_{C_2}$ ). (B) Corresponding normalized reflectance spectra of the iridophores ( $I_1\text{--}I_4$ ) and combined multispectral map of the iridophores only (top right panel). (C) Corresponding normalized reflectance spectra of the chromatophores ( $C_1\text{--}C_2$ ) and combined multispectral map of the chromatophores only (top right panel). Scale bar: 200  $\mu\text{m}$ .

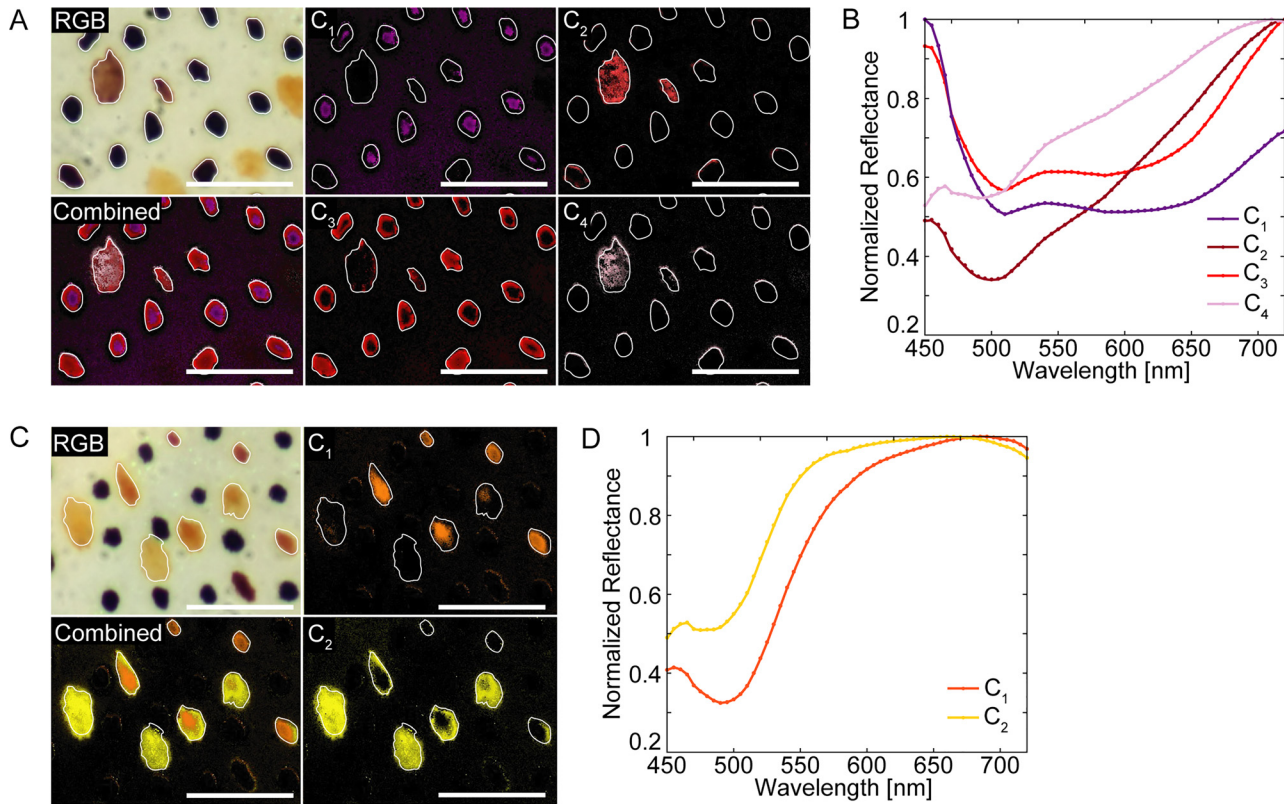


**Figure 3:** Multispectral analysis of pigments density in light and dark chromatophores.

(A) Low magnification multispectral map of aged excised *O. bimaculoides* skin in the spectral range 450–720 nm. The RGB image is spectrally unmixed in false-color images that show the spatial distribution of the dark chromatophores ( $C_1$ – $C_4$ ), as highlighted by the white outline mask, and that can be used to generate the combined multispectral map (Combined). (B) Corresponding normalized reflectance spectra of the dark chromatophores. (C) Low magnification multispectral map of aged excised *O. bimaculoides* skin in the spectral range 450–720 nm. The RGB image is spectrally unmixed in false-color images that show the spatial distribution of the light chromatophores ( $C_1$ – $C_2$ ), as highlighted by the white outline mask, and that can be used to generate the combined multispectral map (Combined). (D) Corresponding normalized reflectance spectra of the light chromatophores. Scale bar: 200  $\mu$ m.

To allow for the acquisition of multispectral maps of freshly excised *O. bimaculoides* skin, the skin was stabilized by immersion in a solution of silk fibroin and glutamate (see Supplementary Material for details), a known neuro-inhibitory agent [6, 41], in addition to being kept wet with artificial sea water (ASW). Silk's known optical clarity [43] allowed to retain the native optical response of both the pigmentary and the structural elements of the octopus skin, thus allowing to properly assign chromatic elements to their optical class (Figure S2). The presence of the silk combined with the glutamate and the artificial sea water was observed to slow down the skin's muscular movement, therefore enabling optical analysis. This behavior is believed to be caused by the formation of a high viscosity silk-based gel activated by the presence of the glutamate and of the ASW [44]. Despite the known effect of glutamate as a chemical able to induce sustained expansion of the chromatophores [6, 41, 42], the opposite behavior was observed for *O. bimaculoides*,

namely a sustained contraction of those organs. No further external stimuli that could induce a controlled dynamic response in the chromatic elements were applied to the skin in the measurements performed.

To spectrally characterize the cephalopod's chromatic elements, multispectral images of freshly excised stabilized skin of *O. bimaculoides* were acquired in a bright field reflection microscope equipped with a multispectral camera operating over a wavelength range  $\Delta\lambda = 450$ –720 nm and acquiring an image every 5 nm (Figure 2) (See Materials and methods for details). As shown by the RGB image of Figure 2(A) the skin exhibits a high density of dark chromatophores ( $C_1$ – $C_2$ ), surrounded by iridophores reflecting in the entire visible range ( $I_1$ – $I_4$ ), with a particularly high density of green reflecting elements. The high proximity of the chromatic elements in the plane of the skin complicates the identification of the spectral response of each individual element. By

acquiring multispectral maps of the skin and by labelling each chromatic element with its reflectance spectrum as a function of wavelength, it is possible to more precisely identify and separate each iridophore and chromatophore class. The RGB images can be “unmixed” into false-color maps that show the spatial distribution of each class of iridophore/chromatophore and of each element of a specific class by assigning a specific color to the spectral band that corresponds to the spectral response of the individual chromatic elements. While this allows to effectively visualize the distribution of similarly behaving spectrally responsive elements, merging of the individual maps ultimately provides an enhanced visual representation of the overall spectral response of the skin (Figure 2(A), Recombined Image) which is useful to visualize the relative arrangement of the disparate classes of chromatic elements and their interplay to provide better insights on the mechanisms of complex coloration that occur in cephalopods *in vivo*.

Specifically, in the stabilized fresh *O. bimaculoides* skin up to four different optical responses could be attributed to iridophores: respectively, the strong and relatively narrow-band reflectance spectra with peaks in the blue ( $I_1$ ), green ( $I_2$ ), yellow ( $I_3$ ), and red ( $I_4$ ) wavelength regions, each identified by the maximum reflectance wavelength, as shown in Figure 2(B). As the illumination and observation angles were kept constant during the multispectral map acquisition, this wide variety of spectral responses is caused either by the presence of iridocytes with different layer thicknesses, thus creating 1D photonic stacks with different stopbands, or by a variation of the orientation of the iridocytes with respect to the skin surface/illumination and observation angles [45]. The iridophores were also observed to be localized mostly in areas surrounding the chromatophores; due to the high absorption of dark chromatophores, iridophores present directly under the chromatophores could be observed only for lightly pigmented chromatophores. Similarly, for pigmentary elements up to two different spectral responses could be identified in fresh stabilized *O. bimaculoides* skin: brown ( $C_1$ ) and orange ( $C_2$ ) reflecting elements, each identified by the minimum reflectance wavelength as reported in Figure 2(C). Notably, the spectral signal corresponding to the reflection from brown chromatophores did not seem to be localized within the brown chromatophores only but could also be found in other regions of the skin; this spectral behavior was consistent with the relatively dark appearance of the skin in highly pigmented regions and is believed to be caused by the presence of dark chromatophores deeper in the skin. Differently from what recently reported for squid [10], no co-localization was observed for structural and pigmentary elements.

### 3.3 Excised aged skin

Spectral maps of were also acquired for aged ( $24 \text{ h} < t_{\text{from excision}} < 48 \text{ h}$ ) *O. bimaculoides* skin samples. These measurements were performed at low magnification both on flat (Figure S3) and curved (Figure S4) skin. Notably, the aged skin did not require chemical stabilization as both the flesh movement and the chromatophores pulsing naturally decayed while also displaying simpler optical responses compared to the fresh skin (Figure 2). These differences can be attributed partly to the natural variation of the arrangement and density of the chromatic elements within the same animal and partly to the degradation of the excised skin [2]. Notably, only one predominant spectral response from the iridophores could be identified on aged *O. bimaculoides* skin, corresponding to a broadband green reflectance (Figures S3b and S4b); the natural decay of the skin is believed to have at least partially compromised the iridocytes stacks, therefore decreasing their relative organization within the iridophores and causing a broadening of the spectral response.

For the aged skin, between two and three different optical responses could be attributed to chromatophores (Figures S3 and S4). The optical response of dark-reflecting chromatophores (orange and brown) from aged skin was consistent with the one previously measured on stabilized fresh skin (Figure 2): in particular they all displayed a reflectance peak centered at ~450 nm followed by a reflectance dip centered at 500/550 nm and by an increasing reflectance for higher wavelengths. Lightly pigmented chromatophores displayed, instead, a strong reflectance shoulder for wavelengths higher than 500 nm ( $C_1$ , Figure S3) consistently with what previously reported also for squid [46].

Besides providing a comprehensive overview of the octopus skin's spectral response, multispectral imaging can provide insights on the response of individual spectral elements of the skin itself. Specifically, chromatophores have a conformation-dependent distribution of pigment granules within them: for punctuated chromatophores the pigment granules are densely packed in the small volume created by the sacculus; on the contrary, for expanded chromatophores, the granules are distributed over a smaller thickness, therefore occupying a larger surface area [7]. Due to the radial arrangement of the muscles around the pigment sacculus a radial distribution of the pigments is expected: a higher density in the center and a progressively lower density towards the edges of the sacculus; conversely this implies a low reflectance intensity from the central area of the chromatophores and a higher reflectance intensity from the edges. This spatial relative density distribution within each pigment

granules can be semiquantitatively monitored using multispectral maps as reported in Figure 3, both for highly pigmented chromatophores (Figure 3(A) and (B)) and for lightly pigmented chromatophores (Figure 3(C) and (D)). In the reported multispectral analysis, the chromatophores size varied between 180 and 1650 pixels (avg = 650 n = 24).

The RGB images can be spectrally unmixed in spectral bands that display a similar variation of the reflectance as a function of the wavelength but with different intensity, which can be attributed to the optical response of different densities of the same type of pigment. As confirmed by the multispectral maps for contracted circular chromatophores, the lowest reflecting areas are usually found in the center of the chromatophores whereas expanded chromatophores show higher irregularity in the location of the lowest reflecting regions, possibly due to a non-perfectly equal pull of the radial muscles that causes uneven distribution of the pigment granules in the sacculus [5].

### 3.4 Color modulation

The relative arrangement of the chromatic elements in the cephalopods' skin is usually described as layered, as reported for some octopus species [47]. Starting from the dermis layer towards the interior, *O. bimaculoides*' skin displays chromatophores, iridophores, and leucophores as schematically represented in Figure 1(D). This implies that the light reflected by the chromatic elements deeper in the skin can be further modulated by the presence of more external elements as shown in Figure 4 and as previously reported also for squid [9]. In practice, the narrowband reflectance generated by the photonic structure of the iridophores can be filtered by the more broadband pigmentary response of the chromatophores if the former lies underneath the latter. The result of this interaction is a broadening of the reflectance peak generated by the structural element for a wavelength range that corresponds to the chromatophores' strongest reflectance spectral range (Figure 4(B)). This strategy allows *O. bimaculoides* to display on the skin color nuances that cannot be generated by the individual chromatic elements, therefore contributing to enriching the broad range of displayed colors and body patterns. This modulation effect can be observed for lightly pigmented chromatophores, as shown by the multispectral maps of Figure 4(A) but was not observed in proximity of darkly pigmented chromatophores. This filtering behavior is expected because of the higher absorption of the dark chromatophores with respect to the lightly pigmented ones.

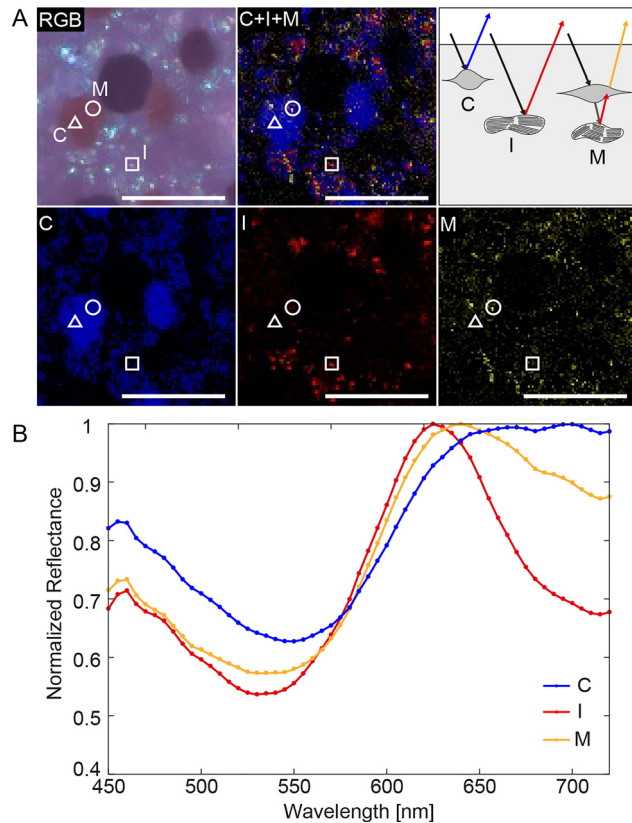


**Figure 4:** Multispectral analysis of color modulation in excised octopus' skin.

(A) High magnification multispectral map of fresh stabilized *O. bimaculoides* skin in the spectral range 450–720 nm. The RGB image is unmixed in false-color images that correspond to the reflectance signal of the chromatophores (C) and of the iridophores (I) individually taken, and of the red iridophores signal modulated by the presence of the brown chromatophores (M). The recombination of the individual spectral bands generates a false-color composite image (C + I + M). The spatial arrangement of the chromatic elements and of their relative optical interference that generates reflectance modulation is schematically depicted in the top right panel. (B) Corresponding normalized reflectance spectra of the red iridophore, the brown chromatophore, and of a red iridophore modulated by the brown chromatophore. The spectra are acquired from the areas delimited by the shapes shown in panel (A) as follows: iridophore – □, chromatophore – △, and modulated – ○. Scale bar: 50 μm.

## 4 Discussion and conclusion

The reported findings underscore the utility of multispectral mapping to gather new quantitative information on the optical response of highly complex natural systems, offering new insights even for widely studied systems such as cephalopod skin. Specifically, multispectral mapping of *O. bimaculoides* was performed both on stabilized fresh skin and on aged skin, thus allowing to evaluate changes in the skin due to tissue variations with time and to generate

spectral maps of the natural variation of the chromatic elements' distribution in the skin. Multispectral mapping demonstrated to be useful for obtaining clear spatial and spectral discrimination between pigmented (chromatophores) and structural (iridophores) chromatic elements in the octopus' skin, in accordance with previously reported micro-spectroscopic analysis for other cephalopods [2, 9, 32]. This type of spectral mapping finds utility in the biooptics study of cephalopods. For instance, since each class of chromatic element could be isolated solely based on their spectral response, this type of classification could be used to determine the hierarchical arrangement of each chromatic component inside a specific body pattern. Body patterns and relative chromatic element arrangements seem to vary among cephalopods species [2], but have not been yet studied from this perspective; the acquisition of multispectral maps, and, especially, the spectral unmixing, would allow checking whether similar chromatic elements arrangements are used by different species to create a specific body pattern. In addition, the dynamic behavior of each chromatic element during the display of specific body patterns could be monitored, leading to the isolation of the individual contribution of each chromatic element class to the overall body pattern. Further, the ability to isolate a chromatic element on the basis of its spectral response could be useful for studying chromatic elements as classes (e.g., dark chromatophores vs light chromatophores vs yellow iridophores) and determine their relative occurrence, arrangement, and development in *in vivo* skin similarly to what recently reported for individual chromatophores in cuttlefish [42].

The pigments' relative density within single chromatophores was then semiquantitatively mapped using multispectral maps both for lightly and darkly pigmented chromatophores, allowing to discriminate between contracted, partially expanded, and fully expanded chromatophores. The use of calibration curves of chromatophores in different expansion states, would allow to quantitatively determine *a priori* the chromatophores punctuation state *in vivo* and nondestructively.

Multispectral mapping also enabled to study the color modulation given by the interplay of structural and pigmented elements, which is central to the richness of cephalopods spectral response. Consistently with what reported for squid [9, 10], the vertical layering of chromatophores and iridophores [46] resulted in a spectral shift and broadening of the reflectance signal generated by the iridophores. In the studied octopus species, the majority of the iridophores are observed in proximity or externally with respect to lightly pigmented chromatophores; as in other cephalopod species this colocalization is much more abundant (e.g., in *Doryteuthis pealeii* squid [10]), multispectral mapping

would be a practical tool to determine the dynamic interplay of structural and pigmentary elements over a large scale (body patterns).

It is envisioned that multispectral mapping will be particularly useful for the study of cephalopod appearance in terms of body patterns (the appearance of the whole animal) and components (the constituents of a pattern) due to the ability to spectrally isolate each chromatic element (the chromatic organs in the skin) [2]. This work aims at being a proof-of-concept for the multispectral analysis of cephalopods skin; in particular, further analysis at skin taken from different areas of the octopus body (e.g., mantle and suckers) could be used to study the presence of any specialization of the chromatic elements as a function of their location on the skin, while similar mapping on squid and cuttlefish could be useful towards a more comprehensive comparison of the evolution of the optical abilities in these species. In addition, multispectral mapping can quickly and reliably provide information not only on the spectral fingerprint of the individual chromatic elements but also on their topographical distribution on the skin and relative spectral modulation, therefore allowing to build spectral libraries that can be used as a reference for the design and the performance evaluation of bioinspired-counterparts. The ability to describe in detail these natural systems adds utility towards understanding their static and dynamic optical responses for the development of biomimetic systems with camouflage abilities. In particular, biomimetic systems that closely match the cephalopods' natural camouflage abilities in terms of overall displayed pattern, color topographical distribution, covered spectral range, and speed of color variation (~ms) [4], can only be achieved by starting from a detailed understanding of their natural counterparts.

**Acknowledgments:** Any opinions, findings, and conclusions or recommendations expressed in this material are those of the author(s) and do not necessarily reflect the views of the Office of Naval Research. We thank Bret Grasse for helpful discussions and Dr. Chuck Winkler (Aquatic Research Consultants) for procuring the live *Octopus bimaculoides* for our research.

**Author contributions:** G.G., M.L. J.F., and F.G.O. designed research. G.G. performed multispectral mapping. G.L. handled animals. G.M prepared silk fibroin. G.M and G.L. helped with *ex vivo* tissue stabilization. G.G. and F.G.O. analyzed data. G.G. and F.G.O. co-wrote the paper. All the authors discussed the results and commented on the paper.

**Research funding:** We would like to gratefully acknowledge support from the Department of the Navy, Office of Naval Research (ONR) under grant number N00014-18-1-2631.

**Conflict of interest statement:** The authors declare no conflicts of interest.

**Data availability:** All data needed to evaluate the conclusions in the paper are present in the paper and/or the Supplementary Materials. Additional data related to this paper may be requested from the authors.

## References

- [1] S. Kinoshita, *Structural Colors in the Realm of Nature*, vol. 368, Singapore, Hackensack, NJ, World Scientific, 2010.
- [2] R. T. Hanlon and J. B. Messenger, *Cephalopod Behaviour*, 2nd ed. Cambridge, UK, Cambridge University Press, 2018.
- [3] P. T. Gonzalez-Bellido, A. T. Scaros, R. T. Hanlon, and T. J. Wardill, "Neural control of dynamic 3-dimensional skin papillae for cuttlefish camouflage," *iScience*, vol. 1, pp. 24–34, 2018.
- [4] R. Hanlon, "Cephalopod dynamic camouflage," *Curr. Biol.*, vol. 17, pp. R400–R404, 2007.
- [5] R. A. Cloney and E. Florey, "Ultrastructure of cephalopod chromatophore organs," *Z. für Zellforsch. Mikrosk. Anat.*, vol. 89, pp. 250–280, 1968.
- [6] J. B. Messenger, "Cephalopod chromatophores: neurobiology and natural history," *Biol. Rev. Camb. Phil. Soc.*, vol. 76, pp. 473–528, 2001.
- [7] L. F. Deravi, A. P. Magyar, S. P. Sheehy, et al., "The structure-function relationships of a natural nanoscale photonic device in cuttlefish chromatophores," *J. R. Soc. Interface*, vol. 11, 2014, <https://doi.org/10.1098/rsif.2013.0942>.
- [8] G. R. R. Bell, A. M. Kuzirian, S. L. Senft, L. M. Mäthger, T. J. Wardill, and R. T. Hanlon, "Chromatophore radial muscle fibers anchor in flexible squid skin," *Invertebr. Biol.*, vol. 132, pp. 120–132, 2013.
- [9] L. M. Mäthger and R. T. Hanlon, "Malleable skin coloration in cephalopods: selective reflectance, transmission and absorbance of light by chromatophores and iridophores," *Cell Tissue Res.*, vol. 329, pp. 179–186, 2007.
- [10] T. L. Williams, S. L. Senft, J. Yeo, et al., "Dynamic pigmentary and structural coloration within cephalopod chromatophore organs," *Nat. Commun.*, vol. 10, p. 1004, 2019.
- [11] S. R. Dinneen, R. M. Osgood, M. E. Greenslade, and L. F. Deravi, "Color richness in cephalopod chromatophores originating from high refractive index biomolecules," *J. Phys. Chem. Lett.*, vol. 8, pp. 313–317, 2017.
- [12] E. J. Denton and M. F. Land, "Mechanism of reflexion in silvery layers of fish and cephalopods," *Proc. R. Soc. Lond. Ser. B Biol. Sci.*, vol. 178, pp. 43–61, 1971.
- [13] W. J. Crookes, L. L. Ding, Q. L. Huang, J. R. Kimbell, J. Horwitz, and M. J. HcFall-Ngai, "Reflectins: the unusual proteins of squid reflective tissues," *Science (80-.)*, vol. 303, pp. 235–238, 2004.
- [14] L. M. Mäthger, S. L. Senft, M. Gao, et al., "Bright white scattering from protein spheres in color changing, flexible cuttlefish skin," *Adv. Funct. Mater.*, vol. 23, pp. 3980–3989, 2013.
- [15] R. T. Hanlon, L. M. Mäthger, G. R. R. Bell, A. M. Kuzirian, and S. L. Senft, "White reflection from cuttlefish skin leucophores," *Bioinspiration Biomimetics*, vol. 13, p. 035002, 2018.
- [16] R. T. Forsythe and J. W. Hanlon, "Behaviour body patterning and reproductive biology of *Octopus bimaculoides* from California," *Malacologia*, vol. 29, pp. 41–55, 1988.
- [17] M. D. Norman and F. G. Hochberg, "The current status of octopus taxonomy," *Phuket Mar. Biol. Cent. Res. Bull.*, vol. 66, pp. 127–154, 2005.
- [18] G. E. Pickford and B. H. McConaughey, "The *Octopus bimaculatus* problem: A study in sibling species," *Bull. Bingham Oceanogr. Collect.*, vol. XII, pp. 1–65, 1949.
- [19] J. W. Forsythe and R. T. Hanlon, "Effect of temperature on laboratory growth, reproduction and life span of *Octopus bimaculoides*," *Mar. Biol.*, vol. 98, pp. 369–379, 1988.
- [20] R. T. Hanlon and J. W. Forsythe, "Advances in the laboratory culture of octopuses for biomedical research," *Lab. Anim. Sci.*, vol. 35, no. 1, pp. 33–40, 1985.
- [21] M. K. Stoskopf and B. S. Oppenheim, "Anatomic features of *Octopus bimaculoides* and *Octopus digueti*," *J. Zoo Wildl. Med.*, vol. 27, 1996.
- [22] J. A. Cigliano, "Dominance and den use in *Octopus bimaculoides*," *Anim. Behav.*, vol. 46, pp. 677–684, 1993.
- [23] R. P. Peterson, "The anatomy and histology of the reproductive systems of *Octopus bimaculoides*," *J. Morphol.*, vol. 104, pp. 61–87, 1959.
- [24] E. B. L. Kennedy, K. C. Buresch, P. Boinapally, and R. T. Hanlon, "Octopus arms exhibit exceptional flexibility," *Sci. Rep.*, vol. 10, p. 20872, 2020.
- [25] C. B. Albertin, O. Simakov, T. Mitros, et al., "The octopus genome and the evolution of cephalopod neural and morphological novelties," *Nature*, vol. 524, pp. 220–224, 2015.
- [26] S. C. Torres, J. L. Camacho, B. Matsumoto, R. T. Kuramoto, and L. J. Robles, "Light-/dark-induced changes in rhabdom structure in the retina of *Octopus bimaculoides*," *Cell Tissue Res.*, vol. 290, pp. 167–174, 1997.
- [27] M. D. Walderon, K. J. Nolt, R. E. Haas, et al., "Distance chemoreception and the detection of conspecifics in *Octopus bimaculoides*," *J. Molluscan Stud.*, vol. 77, pp. 309–311, 2011.
- [28] D. L. Sinn, N. A. Perrin, J. A. Mather, and R. C. Anderson, "Early temperamental traits in an octopus (*Octopus bimaculoides*)," *J. Comp. Psychol.*, vol. 115, pp. 351–364, 2001.
- [29] L. M. Hvorecny, J. L. Grudowski, C. J. Blakeslee, et al., "Octopuses (*Octopus bimaculoides*) and cuttlefishes (*Sepia pharaonis*, *S. officinalis*) can conditionally discriminate," *Anim. Cognit.*, vol. 10, pp. 449–459, 2007.
- [30] J. G. Boal, A. W. Dunham, K. T. Williams, and R. T. Hanlon, "Experimental evidence for spatial learning in octopuses (*Octopus bimaculoides*)," *J. Comp. Psychol.*, vol. 114, pp. 246–252, 2000.
- [31] J. Boal, "Complex learning in octopus-bimaculoides," *Am. Malacol. Bull.*, vol. 9, pp. 75–80, 1991.
- [32] M. Desmond Ramirez and T. H. Oakley, "Eye-independent, light-activated chromatophore expansion (LACE) and expression of phototransduction genes in the skin of *Octopus bimaculoides*," *J. Exp. Biol.*, vol. 218, pp. 1513–1520, 2015.
- [33] C. C. Chiao, J. K. Wickiser, J. J. Allen, B. Genter, and R. T. Hanlon, "Hyperspectral imaging of cuttlefish camouflage indicates good color match in the eyes of fish predators," *Proc. Natl. Acad. Sci. U. S. A.*, vol. 108, pp. 9148–9153, 2011.
- [34] G. Guidetti, H. Sun, B. Marelli, and F. G. Omenetto, "Photonic paper: multiscale assembly of reflective cellulose sheets in *Lunaria annua*," *Sci. Adv.*, vol. 6, p. eaba8966, 2020.

- [35] R. T. Hanlon, C. C. Chiao, L. M. Mäthger, and N. J. Marshall, “A fish-eye view of cuttlefish camouflage using in situ spectrometry,” *Biol. J. Linn. Soc.*, vol. 109, pp. 535–551, 2013.
- [36] J. L. Reid, “The shallow salinity minima of the Pacific Ocean,” *Deep. Res. Oceanogr. Abstr.*, vol. 20, pp. 51–68, 1973.
- [37] D. N. Rockwood, R. C. Preda, T. Yücel, X. Wang, M. L. Lovett, and D. L. Kaplan, “Materials fabrication from *Bombyx mori* silk fibroin,” *Nat. Protoc.*, vol. 6, pp. 1612–1631, 2011.
- [38] G. Fiorito, A. Affuso, J. Basil, et al., “Guidelines for the care and welfare of cephalopods in research –A consensus based on an initiative by CephRes, FELASA and the boyd group,” *Lab. Anim.*, vol. 49, pp. 1–90, 2015.
- [39] G. Fiorito, A. Affuso, D. B. Anderson, et al., “Cephalopods in neuroscience: regulations, research and the 3Rs,” *Invertebr. Neurosci.*, vol. 14, pp. 13–36, 2014.
- [40] V. M. Lopes, E. Sampaio, K. Roumbedakis, et al., “Cephalopod biology and care, a COST FA1301 (CephInAction) training school: anaesthesia and scientific procedures,” *Invertebr. Neurosci.*, vol. 17, p. 8, 2017.
- [41] Q. Bone and J. V. Howarth, “The role of l-glutamate in neuromuscular transmission in some molluscs,” *J. Mar. Biol. Assoc. U. K.*, vol. 60, pp. 619–626, 1980.
- [42] S. Reiter, P. Hülsdunk, T. Woo, et al., “Elucidating the control and development of skin patterning in cuttlefish,” *Nature*, vol. 562, pp. 361–366, 2018.
- [43] B. D. Lawrence, M. Cronin-Golomb, I. Georgakoudi, D. L. Kaplan, and F. G. Omenetto, “Bioactive silk protein biomaterial systems for optical devices,” *Biomacromolecules*, vol. 9, pp. 1214–1220, 2008.
- [44] M. A. Serban and D. L. Kaplan, “PH-sensitive ionomeric particles obtained via chemical conjugation of silk with poly(amino acid)s,” *Biomacromolecules*, vol. 11, pp. 3406–3412, 2010.
- [45] S. Kinoshita, S. Yoshioka, and J. Miyazaki, “Physics of structural colors,” *Rep. Prog. Phys.*, vol. 71, 2008, <https://doi.org/10.1088/0034-4885/71/7/076401>.
- [46] R. L. Sutherland, L. M. Mäthger, R. T. Hanlon, A. M. Urbas, and M. O. Stone, “Cephalopod coloration model I Squid chromatophores and iridophores,” *J. Opt. Soc. Am. A*, vol. 25, p. 588, 2008.
- [47] A. Packard and G. Sanders, “What the octopus shows to the world,” *Endeavour*, vol. 28, pp. 92–98, 1969.

---

**Supplementary Material:** The online version of this article offers supplementary material (<https://doi.org/10.1515/nanoph-2021-0102>).